# Lymphopenia drives T cell exhaustion in immunodeficient STING gain-of-function mice

Damien Freytag [a], Stéphane Giorgiutti [a,b], Nadège Wadier [a], Sabine Depauw [a], Grégoire Hopsomer [a], Philippe Mertz [a], Fabrice Augé [c], Raphaël Carapito [d], Isabelle Couillin [e], Anne-Sophie Korganow [a,b], Francesca Pala [f], Marita Bosticardo [f], Luigi D. Notarangelo [f], Frédéric Rieux-Laucat [g], Nicolas Riteau [e,h], Peggy Kirstetter [i], Pauline Soulas-Sprauel [a,b,*]

[*] Corresponding author: e-mail address: soulaspa@unistra.fr (P. Soulas-Sprauel); postal address: Inserm U1109, CRBS, 1 rue Eugène Boeckel, F-67000 Strasbourg, France.

**Affiliations:**

[a] Laboratoire d'ImmunoRhumatologie Moléculaire, INSERM UMR_S1109, F-67000 Strasbourg, France; Strasbourg University, Faculty of Pharmacy and Faculty of Medicine, Strasbourg, France.

[b] Department of Clinical Immunology and Internal Medicine, National Reference Center for Systemic Autoimmune Diseases (CNR RESO), Tertiary Center for Primary Immunodeficiency, Strasbourg University Hospital, F-67000 Strasbourg, France.

[c] IBMC, Institut de Biologie Moléculaire et Cellulaire, F-67000 Strasbourg, France.

[d] Laboratoire d'ImmunoRhumatologie Moléculaire, Plateforme GENOMAX, INSERM UMR_S 1109, Faculté de Médecine, Fédération Hospitalo-Universitaire OMICARE, ITI TRANSPLANTEX NG, Strasbourg Federation of Translational Medicine (FMTS), Strasbourg University, Strasbourg 67091, France

[e] Experimental and Molecular Immunology and Neurogenetics Laboratory, University of Orleans, Centre National de la Recherche Scientifique (CNRS), UMR7355, 45100 Orleans, France.

[f] Laboratory of Clinical Immunology and Microbiology, National Institute of Allergy and Infectious Diseases (NIAID)/NIH, Bethesda, MD, USA.

[g] Université Paris Cité, Laboratoire d'immunogénétique des maladies auto-immunes pédiatriques, Institut Imagine, INSERM UMR_S1163, Paris, France.

[h] Immune Health Laboratory, 'Regulation of host responses and immune health' IRL2029, French National Centre for Scientific Research (CNRS) and Ribeirão Preto Medical School (FMRP) of the São Paulo University (USP).

[i] Université de Strasbourg, IGBMC UMR 7104- UMR-S 1258, F-67400 Illkirch, France; IGBMC, Institut de Génétique et de Biologie Moléculaire et Cellulaire, F-67400 Illkirch, France.

**Classification:** Biological Sciences – Immunology and Inflammation

**Keywords:**

STING, T cell exhaustion, Lymphopenia, Homeostasis

## Abstract

STING gain-of-function (GOF) mutations are associated with the severe autoinflammatory disease designated STING Associated Vasculopathy with onset in Infancy (SAVI). Mice with the STING GOF V154M mutation develop profound T cell lymphopenia, partly due to a blockage of T cell development in the thymus. To better characterize the mechanisms of peripheral T cell dysfunctions, we conducted a transcriptomic and phenotypic analysis on sorted splenic CD4+ and CD8+ mature T cells from STING GOF V154M mice. We identify a T cell exhaustion phenotype that manifests at a terminal stage, acquired early in life but only after reaching the peripheral environment. This phenotype is independent of type I interferons and

does not rely on intrinsic STING activation in either T cells or stromal cells. Mechanistically, the limited number of mature T cells that reach the periphery appear to be quickly impacted by the lymphopenic environment, experiencing heightened stimulation of the IL-7 receptor and TCR pathways, including the NFAT pathway, a key factor in T cell exhaustion. By performing transplantation experiments with STING GOF long term-hematopoietic stem cells (LT-HSCs) along with supportive wild-type bone marrow (BM) cells, we were able to prevent the T cell exhaustion of STING GOF T cells in the resulting non-lymphopenic context, demonstrating that lymphopenia is a major driver of T cell exhaustion in STING GOF mice. T cell exhaustion, although less severe, was also observed in lymphopenic mice carrying *Rag1* hypomorphic mutations. In conclusion, our results, which highlight T cell exhaustion induced by lymphopenia, could have important implications for the management of patients with severe immune deficiencies.

**Highlights**

- We describe a phenotype of T cell exhaustion in STING GOF V154M mice, which is acquired early in life and in the periphery.
- STING GOF-associated T cell exhaustion is independent of type I IFNs, and STING GOF/activation in T cells or in stromal cells is not sufficient for T cell exhaustion.
- Lymphopenia is a major driver of T cell exhaustion in STING GOF mice, and increased antigenic/IL-7 stimulation of T cells in the lymphopenic context of STING GOF mice could be implicated in the induction of T cell exhaustion.

72 **Introduction**

73 Stimulator of Interferon Genes (STING) belongs to cytosolic double-stranded-DNA-
74 sensing pathways in innate immunity and has emerged as a central player in antiviral,
75 antibacterial, and anti-tumor immunity (1). When activated by cyclic dinucleotides produced
76 by cyclic GMP-AMP synthase (cGAS), STING translocates from endoplasmic reticulum (ER)
77 to ER-Golgi intermediate compartment (ERGIC)/Golgi where it activates TANK-binding
78 kinase 1 (TBK1), which then phosphorylates interferon regulatory factor 3 (IRF3) and induces
79 the expression of type I interferons (IFNs). In turn, type I IFNs activate the type I IFNs receptor
80 (IFNAR), inducing the expression of a set of interferon-stimulated genes (ISG) and triggering
81 inflammation. The NF-kB pathway is also engaged following STING activation, participating
82 in the inflammatory response (2).

83 Heterozygous gain-of-function (GOF) mutations in STING-coding gene *STING1* lead
84 to constitutive activation of the protein and have been described in patients with an
85 autoinflammatory disease designated STING Associated Vasculopathy with onset in Infancy
86 (SAVI) (3, 4), classified as a type I interferonopathy, with increased ISGs expression (5). This
87 disease is associated with damages to the skin small blood vessels and an interstitial lung
88 disease at the origin of morbidity and mortality (6–8). To study the role of STING in the
89 pathophysiology of the disease, our team (9) and others (10–16) developed STING GOF mouse
90 models including mice carrying the heterozygous V154M mutation (9, 10), corresponding to
91 the most common human V155M mutation (about 60%) in SAVI patients. STING GOF V154M
92 mouse models develop type I IFN-independent auto-inflammatory manifestations, notably lung
93 disease (10, 17), and also a high decrease of T cell counts in a context of severe combined
94 immunodeficiency (SCID) (9, 10), reminiscent of T cell lymphopenia cases among SAVI
95 patients. T cell lymphopenia was also described in STING GOF N153S models (10, 11). In

96 STING GOF N153S and V154M mice, the T cell lymphopenia is partly explained by an
97 impairment of T cell development at double negative (DN)1 and DN2 stages (9, 11).
98 In addition, we showed that the rare mature T cells found in the periphery exhibited both
99 defective proliferation and increased apoptosis, which maintain the lymphopenic state (9).
100 These defects are at least partly STING-intrinsic as its anti-proliferative effect was confirmed
101 in human T cells overexpressing the STING GOF V155M mutant (18). In addition, a pro-
102 apoptotic effect of STING in lymphocytes was also reported in other models, and involves
103 TBK1 (19), endoplasmic reticulum (ER) stress (20) or p53-dependent pathways (21). However,
104 treatment of STING N153S mice with a pan-caspase inhibitor or ER stress blocker only
105 partially reverse T cell lymphopenia (20). Thus, other mechanisms must explain the functional
106 defects of peripheral T cells and maintenance of lymphopenia in STING GOF mice.
107 To better characterize these mechanisms, we perform in the present study a
108 transcriptomic analysis on sorted T cells from STING GOF mice compared to their wild-type
109 (WT) littermate controls. An enrichment of transcriptomic signatures associated with T cell
110 exhaustion is revealed and confirmed by the overexpression of key transcription factors and
111 several surface inhibitory receptors (like PD-1, TIGIT, TIM-3 and LAG-3). We further
112 demonstrate that T cell exhaustion is associated with enhanced TCR (including NFAT
113 signaling) and IL-7R signaling in the lymphopenic environment. Importantly, we do not
114 observe any sign of T cell exhaustion in STING GOF T cells developing in non-lymphopenic
115 mice. Finally, a similar T cell exhaustion phenotype (albeit less severe than in STING GOF
116 mice) is observed in other lymphopenic conditions, as shown in mice carrying hypomorphic
117 mutations of *Rag1* gene (22). Together, these observations demonstrate that T cell exhaustion
118 phenotype in STING V154M mice is mostly triggered by lymphopenia and likely reinforce this
119 lymphopenia by a self-maintaining loop. While T cell exhaustion has primarily been described
120 as a consequence of chronic T cell stimulation in the context of persistent infections and cancers

121 (23, 24), our study reveals that lymphopenia should also be considered as a context that can
122 trigger T cell exhaustion, echoing recent findings of T cell exhaustion in patients with severe
123 combined immunodeficiencies (SCID) (25, 26).

124 **Results**

125

126 **CD4$^+$ and CD8$^+$ T cells from STING GOF mice display an exhausted phenotype, acquired**
127 **in the periphery in a type I IFN independent manner**

128 Mice carrying the heterozygous STING V154M mutation are characterized by a SCID
129 phenotype associated with marked T cell dysfunctions, including impaired proliferation, and
130 enhanced apoptosis (9). To decipher the mechanisms underlying this phenotype, we performed
131 a transcriptomic analysis by RNA-seq on sorted splenic CD4$^+$ and CD8$^+$ T cells from STING
132 GOF mice compared to their WT littermate controls. This analysis revealed a transcriptomic
133 signature of T cell exhaustion in CD4$^+$ and CD8$^+$ T cells in the STING GOF group, as shown
134 by a negative enrichment of the transcripts upregulated in naive versus exhausted T cells, as
135 well as a positive enrichment of the genes downregulated in naive versus exhausted T cells
136 (GSE9650 (27)) (**Fig. 1A**). T cell exhaustion is an altered differentiation state of chronically
137 activated T cells, notably caused by persistent antigenic stimulation and sustained
138 inflammation, and is commonly occurring in chronic viral infections or cancers (23, 24).
139 Exhausted T cells co-express inhibitory receptors (like PD-1, TIGIT, TIM-3 and LAG-3) in a
140 sustained manner (24). Furthermore, exhausted T cells progressively lose their proliferative and
141 effector functions, which is reminiscent of the functional defects of mature STING GOF T cells
142 (9, 10).

143 Analysis of gene expression for key transcription factors associated with T cell
144 exhaustion in STING GOF T cells revealed overexpression of *Nfatc1 and Nfatc2* compared to
145 WT cells, without concurrent induction of the AP-1 cofactors *Fos* and *Jun* (**Fig. 1B**). This
146 pattern is indicative of a preferential activation of the transcriptional program of exhaustion
147 (28). We also observed increased expression of T cell exhaustion-associated transcription
148 factors, like EOMES (*Eomes*) and T-BET (*Tbx21*), as well as TOX (*Tox*), the latter being more

149 involved in the most advanced stages of T cell exhaustion program (**Fig. 1B**). Moreover,
150 transcripts of multiple genes encoding for inhibitory receptors (*Pdcd1*, *Tigit*, *Havcr2*, *Lag3*,
151 *Cd244*, *Entpd1*, *Ctla4* and *Cd160*) were also overexpressed (**Fig. 1C**). Accordingly, the
152 percentages of splenic $CD4^+$ and $CD8^+$ T cells positive for PD-1, TIGIT, TIM-3 or LAG-3
153 expression were significantly increased in STING GOF mice compared to their WT controls
154 (**Fig. 1D**). Then, we analyzed the expression of additional markers to define more precisely the
155 exhaustion stage of T cells in STING GOF mice. As *Tcf7* transcript was downregulated in our
156 RNA-seq data (**Fig. 1B**), we hypothesized that STING GOF T cells could be terminally
157 exhausted. We analyzed co-expression of the inhibitory receptors PD-1 and TIM-3, as well as
158 the transcription factor TCF-1 (encoded by *Tcf7* gene), to identify progenitor exhausted (PE) T
159 cells (PD-$1^+$TCF-$1^+$TIM-$3^-$) and terminally exhausted (TE) T cells (PD-$1^+$TCF-$1^-$TIM-$3^+$) (29).
160 An increased proportion of TE T cells was observed among $CD4^+$ and $CD8^+$ T cells from
161 STING GOF mice as compared to control mice. Interestingly, the STING GOF T cell
162 exhaustion phenotype appeared to be more profound in $CD4^+$ than in $CD8^+$ T cells (**Fig. 1E**).
163 Together, our findings revealed an unexpected phenotype of T cell exhaustion in STING GOF
164 mice, which reaches the stage of terminal exhaustion, and might contribute to the T cell
165 dysfunctions described in these mice.

166 Given that STING V154M mice develop a lung disease partly mediated by T cells (17),
167 we also investigated potential T cell exhaustion in the lungs. Interestingly, as in the spleen, the
168 proportion of $CD4^+$ and $CD8^+$ T cells infiltrating the lungs that expressed PD-1 (data available
169 for $CD4^+$ T cells), TIGIT, TIM-3 or LAG-3 was significantly higher in STING GOF mice
170 compared to WT controls (**Fig. S1A**).

171 To determine if this exhaustion phenotype has a central origin, we examined whether
172 the single positive (SP) T cells, the most terminally differentiated T cell progenitors in the
173 thymus, were already exhibiting the phenotype. We observed only minimal increase of cells

174 expressing inhibitory receptors, for both thymic SP $CD4^+$ and $CD8^+$ progenitors (**Fig. S1B**). In
175 contrast, we demonstrated that splenic T cells from very young (2-week-old) mice, which
176 represent cells that have just left the thymus for the periphery, were already displaying the
177 exhaustion phenotype of adult mice (**Fig. S1C**). Altogether, these results demonstrate that the
178 T cell exhaustion phenotype in STING GOF mice is acquired very early after birth, but only
179 once T cells have reached the periphery.

180 Since STING drives type I IFNs, which have recently shown to regulate coinhibitory
181 receptors expression on T cells (30), we then explored the role of these cytokines in T cell
182 exhaustion in STING GOF mice. Overall, the T cell exhaustion phenotype was not reversed by
183 IFNAR deficiency in STING GOF mice (**Fig. S2**).

184

185 **$Ca^{2+}$-NFAT pathway is activated by STING, but is not sufficient to induce T cell**
186 **exhaustion**

187 We then searched for signals that could induce the exhaustion phenotype in STING GOF
188 T cells. Considering its crucial role in T cell exhaustion (31) and its upregulation in our RNA-
189 seq data (**Fig. 1B**), we first focused on NFAT signaling pathway.

190 Transcriptomic analysis confirmed a significant enrichment of NFAT signature from
191 the Pathway Interaction Database (PID) in STING GOF T cells, compared to control T cells
192 (**Fig. S3A**). Upregulation of the total (nuclear and cytosolic) NFATc1 transcription factor
193 expression was confirmed by flow cytometry (**Fig. S3B**). NFAT activation relies on its
194 dephosphorylation by the calcium ($Ca^{2+}$)-calmodulin-calcineurin pathway, and $Ca^{2+}$
195 homeostasis is known to be disrupted in STING GOF T cells (20). Using Fura Red™-mediated
196 ratiometric measurement to study basal $Ca^{2+}$ levels, we demonstrated that basal $Ca^{2+}$ levels were
197 higher in $CD4^+$ and $CD8^+$ T cells from STING GOF mice compared to their WT controls,

198 suggesting that $Ca^{2+}$-NFAT signaling pathway in STING GOF T cells participates to the
199 induction of their exhaustion (**Fig. S3C**).

200 We next wondered whether the activation of the $Ca^{2+}$-NFAT signaling pathway could
201 be due to the STING activation *per se*. Therefore, we treated WT splenocytes with STING
202 agonist 5,6-dimethylxanthenone-4-acetic acid (DMXAA) *in vitro*. After 4 hours, DMXAA-
203 treated $CD4^+$ and $CD8^+$ T cells presented an increase of their basal $Ca^{2+}$ levels, similar to those
204 observed in untreated STING GOF T cells (**Fig. 2A**). After 24 hours, DMXAA-treated cells
205 also showed upregulation of NFATc1 to the same extent as untreated STING GOF T cells (**Fig.**
206 **2B**). However, STING activation *in vitro* was not sufficient to induce an increase of key
207 inhibitory receptors PD-1 and TIM-3 (**Fig. 2C**).

208 In conclusion, even if it can contribute to the $Ca^{2+}$-NFAT activation, STING activation
209 in T cells is not sufficient to induce their exhaustion, reinforcing the importance of an
210 environmental factor that was already suggested comparing thymic versus splenic exhaustion
211 profile from 2-weeks old STING GOF mice (**Fig. S1C**).

212

213 **STING GOF T cells displayed features of TCR and IL-7R engagement mediated by the**
214 **lymphopenic environment**

215 We then hypothesized that NFAT activation in STING GOF could be the consequence
216 of TCR signaling secondary to antigenic stimulations (31). Indeed, beyond NFAT
217 overexpression, transcriptomic analysis confirmed a significant enrichment of a broader TCR
218 signaling pathway signature from the Wikipathways (WP) in STING GOF T cells compared to
219 control T cells (**Fig. 3A**). In addition, we highlighted a significant downregulation of CD3
220 expression (consistent with TCR stimulation) on the surface of STING GOF T cells compared
221 to control T cells (**Fig. 3B**).

222 This antigenic stimulation was not secondary to an acute or chronic infection status, as
223 STING GOF mice were bred and held under specific opportunist pathogen free (SOPF)
224 environment, and was not associated with cancer as no tumors were detected in these mice.
225 Thus, we hypothesized that increased TCR stimulation by conventional dendritic cells (cDCs)
226 could be responsible for this phenotype, similar to what is observed during homeostatic
227 proliferation of T cells in lymphopenic environments, promoting the reconstitution of the
228 lymphoid compartment in the periphery (32). Interestingly, we showed a much higher number
229 of cDCs per $CD4^+$ T cell, and, to a lesser extent per $CD8^+$ T cell, in STING GOF mice compared
230 to their WT controls, which could enhance antigen-mediated TCR activation (**Fig. 3C**).
231 Besides antigenic stimulation, IL-7 could also affect T cell fate in STING GOF T-cell
232 lymphopenic environment, since IL-7R engagement promote T cell homeostatic proliferation
233 (32). A marked down-regulation of the alpha chain of the receptor (IL-7Rα), reminiscent of IL-
234 7R engagement, was observed for both $CD4^+$ and $CD8^+$ T cells (**Fig. 3D**). IL-7Rα expression
235 was already significantly downregulated in $CD4^+$ and $CD8^+$ naive T cells from STING GOF
236 mice (**Fig. 3E**), indicating that T-cell lymphopenia impacts T cell fate at early stage in the
237 periphery of STING GOF mice.
238 Taken together, our results suggest that the lymphopenic environment impacts T cells
239 in STING GOF mice through TCR and IL-7R engagement, which are known to govern
240 lymphopenia-induced homeostatic proliferation.
241
242 **T cell exhaustion phenotype of STING GOF T cell is reversed in a non-lymphopenic**
243 **environment**
244 We next wondered whether STING GOF T cells would display an exhausted profile in
245 a non-lymphopenic context. To this purpose, we took advantage of bone marrow transplantation
246 experiments. We sorted long term-hematopoietic stem cells (LT-HSCs) from bone marrow

247 (BM) of donor STING GOF or WT littermate control mice (CD45.2$^+$, donor) and co-
248 transplanted them along with supportive WT BM cells (CD45.1$^+$, support) into irradiated WT
249 recipient mice (CD45.1$^+$CD45.2$^+$, host) (**Fig. 4A**). First, we confirmed the hematopoietic
250 intrinsic effect of the STING GOF mutation on splenic T cell reconstitution (10), as very few
251 T cells were derived from the STING GOF LT-HSCs (red dots), while reconstitution was
252 effective from WT LT-HSCs (black dots). However, the lack of T cell reconstitution from the
253 STING GOF LT-HSCs was compensated by transplantation of supportive WT BM-derived T
254 cells (grey dots) (**Fig 4B**). Consequently, absolute numbers of total (including both CD45.1$^+$
255 and CD45.2$^+$) CD4$^+$ and CD8$^+$ T cells were similar in STING GOF (STING GOF→WT) and
256 WT LT-HSCs (WT→WT) transplantation settings (**Fig 4C**). Interestingly, STING GOF LT-
257 HSCs-derived CD4$^+$ and CD8$^+$ T cells did not overexpress the inhibitory receptors PD-1,
258 TIGIT, TIM-3 or LAG-3 when compared to WT LT-HSCs-derived T cells, or to WT supportive
259 BM-derived T cells (**Fig 4D**). Consistent with this, there were no terminally exhausted (TE) T
260 cells among STING GOF LT-HSC-derived CD4$^+$ and CD8$^+$ T cells (**Fig 4E**).

261 Nevertheless, because of the WT background of recipient mice in LT-HSC
262 transplantations, radio-resistant stroma was composed of WT cells (**Fig 4A**), which is not the
263 case in STING GOF mice. In order to determine the potential impact of the STING GOF stroma
264 on the T cell exhaustion phenotype, we performed transplantation experiments in which total
265 BM cells from WT donor mice (CD45.1$^+$, donor) were transplanted into STING GOF or WT
266 irradiated recipient mice (CD45.2$^+$, host) (**Fig. S4A**). As expected, a good splenic T-cell
267 reconstitution were observed upon transplantation of WT donor BM cells into STING GOF
268 irradiated host (**Fig. S4B**). In addition, the absolute numbers of CD4$^+$ and CD8$^+$ T cells were
269 comparable in the two groups (WT→WT, and WT→STING GOF) of mice (**Fig. S4C**).
270 Moreover, the proportion of CD4$^+$ and CD8$^+$ T cells expressing the inhibitory receptors PD-1,
271 TIGIT, TIM-3 or LAG-3 was similar following transplantation of WT donor BM cells into

272 irradiated STING GOF mice or WT recipients (**Fig. S4D**), and the proportion of TE T cells was
273 extremely low in either group of mice (**Fig. S4E**).
274 Together, these data indicate that STING GOF stroma does not trigger T cell exhaustion
275 phenotype and rather identify T cell lymphopenia as the main mechanism driving T cell
276 exhaustion in STING GOF mice.
277
278 **Mice carrying Rag1 hypomorphic mutations also display lymphopenia-associated T cell**
279 **exhaustion**
280 In order to determine if lymphopenia-mediated T cell exhaustion in STING GOF mice
281 is specific to the STING GOF mutation, we investigated whether another lymphopenic mouse
282 model might also show T cell exhaustion. To this purpose, we studied two mouse models
283 carrying hypomorphic *Rag1* mutations (*Rag1*$^{R972Q/R972Q}$ and *Rag1*$^{R972W/R972W}$ mice, thereafter
284 referred to as RAG1 R972Q and RAG1 R972W mice), also presenting T cell lymphopenia of
285 central origin, based on early block in T cell development (22) as in STING GOF mice. Indeed,
286 RAG1 R972Q and R972W mutant mice similar levels of $CD4^+$ and $CD8^+$ T cell lymphopenia
287 in spleen, compared to STING GOF mice (**Fig. S5A**).
288 Interestingly, a significant proportion of $CD4^+$ and $CD8^+$ T cells from RAG1 R972Q
289 and R972W mice was expressing inhibitory receptors compared to their WT controls, albeit not
290 to the same extent as observed in STING GOF T mice for the majority of inhibitory receptors
291 studied (**Fig. 5**). TE T cells were also increased among $CD4^+$ and $CD8^+$ T cells for both RAG1
292 mutants compared to their WT controls, without reaching the same proportion as in STING
293 GOF mice (**Fig. S5B**). In conclusion, lymphopenia seems to be sufficient to induce T cell
294 exhaustion. However, as T cell exhaustion appeared to be more severe in STING GOF mice
295 compared to RAG1 hypomorphic mutant mice, additional factors beyond central T cell

296 lymphopenia must contribute to the higher degree of T cell exhaustion observed in STING GOF

297 mice.

298 **Discussion**

299 Our data revealed an unexpected T cell exhaustion phenotype in STING GOF mice.
300 Usually associated with chronic T cell stimulation (as in the case of chronic viral infections and
301 cancers), this altered state of T cell differentiation turned out to be of particular interest since it
302 could account for some of the functional defects of mature STING GOF T cells, especially their
303 lack of proliferation in response to TCR activation (9). Moreover, we show here that T cell
304 exhaustion in STING GOF mice is type I IFN-independent, as was the T cell proliferation defect
305 (9). Overall, T cell exhaustion could contribute to T cell proliferation defects and apoptosis, in
306 addition to intrinsic effects of the STING protein in mature T cells (18–21).

307 T cell exhaustion is also associated with a progressive loss of effector properties. In
308 particular, T cell exhaustion may limit IFN-γ production by T cells, which is known to be
309 increased by STING activation (17, 33) and to contribute to the lung disease mortality (17).
310 Therefore, T cell exhaustion could thus be beneficial in STING GOF mice by limiting tissue
311 immunopathology, similarly to the effect of T cell exhaustion in other auto-inflammatory and
312 autoimmune diseases (34). In accordance with this, we also showed an increased proportion of
313 exhausted T cells in lungs of STING GOF mice.

314 In addition to T cell exhaustion associated with prolonged antigenic stimulations as
315 chronic viral infections or tumoral context (35), we describe here a T cell exhaustion state
316 whose main driver is represented by lymphopenic environment. Like the two other contexts, T
317 cell exhaustion in STING GOF mice appeared to be driven mainly by the environment rather
318 than an intrinsic effect in T cells. Indeed, acute treatment of WT splenocytes with DMXAA *in*
319 *vitro* had a pre-activating effect on T cells without inducing an exhaustion phenotype. In
320 addition, bone marrow transplantation experiments showed that STING GOF LT-HSCs-
321 derived T cells developing in a predominantly WT and non-lymphopenic environment do not
322 manifest the exhaustion phenotype. Among environmental factors potentially implicated in the

323 T cell exhaustion of STING GOF mice, type I IFNs were shown to be dispensable, despite the
324 potential role of these cytokines suggested in the literature (30, 36, 37). When studying other
325 environmental factors, the STING GOF stroma does not appear to be sufficient to induce T cell
326 exhaustion.

327 STING GOF T cells display signs of TCR and IL-7R engagement, consistent with
328 lymphopenia-associated signals provided by (auto)antigen and IL-7-mediated stimulation,
329 respectively. While these signals are known to lead to generation of memory-like T cells
330 through homeostatic proliferation (32), T cell exhaustion appeared as a new phenomenon,
331 presumably linked to the persistency of these signals. Of note, the observation that the
332 lymphopenia leads to a higher number of cDCs per $CD4^+$ T cells than for $CD8^+$ T cells may
333 help explain the more severe T cell exhaustion phenotype observed for $CD4^+$ T cells. Finally,
334 the observation that mice carrying hypomorphic *Rag1* mutations are lymphopenic and display
335 obvious signs of T cell exhaustion further supports the notion that lymphopenia may represent
336 an important mechanism leading to T cell exhaustion.

337 Nevertheless, T cell exhaustion in STING GOF mice appears to be more severe than the
338 one observed in the two RAG1 hypomorphic mutant models studied. This difference does not
339 depend on the severity of the lymphopenia, since the latter was even more profound, especially
340 in the RAG1 R972W mutant. Thus, the STING GOF mutation may synergize with lymphopenia
341 in promoting and aggravating T cell exhaustion. An important contributory mechanism to the
342 phenomenon may be represented by the intrinsic effect of STING on T cell activation, as
343 suggested by the upregulation of $Ca^{2+}$-NFAT pathway upon DMXAA treatment. This NFAT
344 activation had been already highlighted by a previous transcriptomic analysis, also indicating
345 its independence from type I IFN (38). Thus, the STING GOF mutation could place the T cells
346 in a pre-activated state, making them not only more sensitive to endoplasmic reticulum stress
347 and apoptosis (20), but also to exhaustion. Even if we demonstrated that STING GOF

348 radioresistant cells (stroma) do not trigger T cell exhaustion phenotype by themselves,
349 synergistic effects of the STING GOF mutation on the antigen presentation capacity of both
350 non-hematopoietic and hematopoietic cells, especially cDC which are also included in the
351 radioresistant cell population, could reinforce TCR stimulation in the lymphopenic context and
352 thus contribute to exhaustion. The impact of this mutation on major histocompatibility complex
353 (MHC) molecules expression has already been demonstrated in endothelial cells within the lung
354 environment in STING GOF mice (17). Moreover, STING activation by agonists in mice has
355 been associated with the loss of cDC1 (39), a subpopulation that plays a crucial role in
356 maintaining and isolating progenitor exhausted (PE) T cells and preventing their transition into
357 terminally exhausted (TE) T cells (40).

358 Overall, our data show that the T cell exhaustion phenotype in STING V154M mice is
359 the result of poor central production of T cells and will potentially reinforce this lymphopenia
360 by a self-maintaining loop. These data should be considered in the context of severe T cell
361 lymphopenia as severe combined immunodeficiencies (SCID). Importantly, recent descriptions
362 of SCID patients developing T cell exhaustion have reinforced a lymphopenia-mediated T cell
363 exhaustion mechanism (25, 26). In particular, the analysis of 61 SCID patients receiving
364 hematopoietic cell transplantation (HCT) recently showed that patients with poor T cell
365 reconstitution after HCT display an increased frequency of exhausted T cells, compared to
366 patients with normal T cell counts after HCT, therefore directly linking lymphopenia with T
367 cell exhaustion (25). In addition, T cell depletion treatments were identified as an important
368 factor associated with PD1 expression on T cells in patients receiving HCT (41).

369 In conclusion, the data and lessons drawn from the STING GOF mice could therefore
370 be of key importance for the follow up of patients receiving HCT on the one hand, but also for
371 a better comprehension of potential T cell exhaustion in lymphopenic murine models on the

372 other hand. Finally, STING GOF mice constitute a good model for the study of T cell
373 exhaustion in non-infectious and non-tumoral contexts.

374 **Materials and methods**

375 Detailed information on the materials and methods can be found in SI Appendix,
376 Supporting Materials and Methods.

377

378 **Mice and cells**

379 Detailed information on mice and cells can be found in SI Appendix, Supporting
380 Materials and Methods.

381

382 **Flow cytometry and cell sorting**

383 Splenic, thymic, BM or lung single-cell suspensions were analyzed by flow cytometry
384 according to standards protocol. Cells were stained with the antibodies listed in SI Appendix
385 (Supporting Materials and Methods) in PBS (Gibco) supplemented with 2% v/v FBS
386 (Dutscher). Intracellular of total (nuclear and cytosolic) TCF-1 and NFATc1 stainings were
387 performed with anti-TCF-1 AF647 (S33-966, BD Pharmingen) and anti-NFATc1 PE (7A6,
388 BioLegend) antibodies, after fixation and permeabilization of cells using Foxp3/Transcription
389 Factor Staining Buffer Set (Thermo Fisher Scientific), according to the manufacturer's
390 instructions. Viability was assessed by Fixable Viability Dye eFluor™ 450 (eBioscience) or
391 DAPI (1 µM/mL Sigma) stainings. Cells were analyzed using an Attune NxT™ flow cytometer
392 (Thermo Fisher Scientific). Data were analyzed using FlowJo software (TreeStar).

393

394 **RNA-seq on sorted $CD4^+$ and $CD8^+$ T cells**

395 Splenocytes from STING GOF mice (n=5) and WT littermate controls (n=5) were
396 stained as described above with anti-CD3e FITC (clone 145–2 C11, BD Biosciences), anti-CD4
397 AF700 (RM4-5, BD Pharmingen), anti-CD8a PE (53-6 .7, BD Pharmingen) and DAPI (1
398 µM/mL, Sigma) before positive sorting of live $CD3^+CD4^+$ or $CD3^+CD8^+$ T cells using a BD

399 FACSAria™ Fusion flow cytometer (IGBMC Flow Cytometry Facility, Strasbourg, France).
400 Isolated cells were at least 95% pure. Total RNA was extracted using RNeasy® Plus Micro Kit
401 (Qiagen) according to the manufacturer's instructions. RNAseq analyses were performed by
402 the Genomax Facility (INSERM U1109, ImmunoRhumatologie Moléculaire, Université de
403 Strasbourg, France). Libraries were prepared from 10 ng RNA using SMARTer Stranded Total
404 RNA-Seq Kit, Pico Input Mammalian (Takara) following the manufacturer's instructions.
405 Briefly, random primers were used for first-strand synthesis, and ribosomal cDNA was cleaved
406 by ZapR V.2 in the presence of mammalian R-probes V.2. Libraries were pooled and sequenced
407 (paired-end 2×75 bp) on a NextSeq 500 using the NextSeq 500/550 High Output Kit V.2
408 according to the manufacturer's instructions (Illumina). For each sample, quality control was
409 carried out and assessed with the next-generation sequencing (NGS) Core Tools FastQC. Reads
410 were aligned against *Mus musculus* mm10 reference genome using TopHat 2 Aligner (42) and
411 gene expression levels were estimated using Cufflinks V.2.1.1 (43). Differential expression
412 analysis was performed with Cuffdiff V.2.1.1 after exclusion of fragments per kilobase million
413 below 9. Gene Set Enrichment Analysis (GSEA) was carried out according to the developer's
414 recommendations. The STING GOF versus WT FPKMs of all genes detected in the RNA-seq
415 were used for the ranked genes list and compared with the indicated signatures from the
416 Molecular Signatures Database (MSigDB), using GSEA Software (UC San Diego, Broad
417 Institute) (44, 45). Raw RNAseq data have been deposited in the EMBL-EBI ArrayExpress
418 archive (accession no. E-MTAB-13658).
419
420 **Cytosolic $Ca^{2+}$ level measurements**
421 For cytosolic $Ca^{2+}$ level measurements, splenic single-cell suspensions were stained as
422 described above with Fixable Viability Dye eFluor™ 450 (eBioscience), anti-CD4 AF700
423 (RM4-5, BD Pharmingen) and anti-CD8a PE-CD584 (53-6 .7, BD Pharmingen) before being

424 loaded with 2 µM Fura Red™ acetoxymethyl ester (AM) (Thermo Fisher Scientific) in PBS
425 2% FBS containing 0.02% pluronic F-127 (Thermo Fisher Scientific) for 30 min at 37°C,
426 avoiding light. Loaded cells were washed, resuspended in DMEM (Gibco) containing 1.8 mM
427 $Ca^{2+}$ and incubated for 10 min at 37°C avoiding light, before acquisition using an Attune NxT™
428 flow cytometer (Thermo Fisher Scientific). After an initial 50-sec acquisition sequence,
429 ionomycin (1 µg/mL, InvivoGen) was added, as positive control, before the acquisition of a
430 second 60-sec sequence. $Ca^{2+}$ levels were determined according to time by ratiometric analyzes
431 between VL4 (405 nm-excitation; 660 nm-emission) and BL3 (488 nm-excitation; 695 nm-
432 emission) channels using FlowJo software (TreeStar).
433
434 **Splenocyte culture**
435 *In vitro* splenocytes stimulations were performed in complete RPMI-1640 medium
436 containing L-glutamine (Lonza) supplemented with 10% v/v FBS (Dutscher), 50 mmol/L β-
437 mercaptoethanol (Gibco), 1% penicillin/streptomycin (Gibco), and 10 mmol/L HEPES
438 (Lonza). Splenocytes were stimulated for the indicated times at 37°C, under 5% $CO_2$, with the
439 STING agonist 5,6-dimethylxanthenone-4-acetic acid (DMXAA) (10 µg/mL, InvivoGen).
440
441 **LT-HSCs transplantations with supportive BM cells**
442 For LT-HSCs sorting, total BM cells were stained for lineage marker expression with
443 biotinylated anti-CD3 (17A2, BioLegend), anti-CD4 (GK1.5, BioLegend), anti-CD8 (53.6.7,
444 eBioscience), anti-CD11b (M1/70, BioLegend), anti-CD19 (1D3, BioLegend), anti-
445 CD45R/B220 (RA3-6B2, BioLegend), anti-CD49b (DX5, BioLegend), anti-Gr-1 (Ly-6G/C)
446 (RB6-8C5, BioLegend), anti-TER-119 (TER-119, BioLegend), before depletion with
447 Dynabeads sheep anti-rat IgG beads (Thermo Fisher Scientific). Lineage-negative cells were
448 stained as described above with Streptavidin AF700 (Invitrogen), anti-CD48 FITC (HM48-1,

449 BioLegend), anti-CD117 (c-Kit) APC (2B8, BioLegend), anti-CD150 (SLAM) PE (TC15-
450 12F12.2, BioLegend), anti-Sca-1 (Ly-6A/E) PE-Cy7 (D7, BioLegend) and DAPI (1 µM/mL,
451 Sigma) before positive sorting of live LT-HSCs ($CD48^{-}CD150^{+}Lin^{-}Sca1^{+}cKit^{+}$) using a BD
452 FACSAria™ Fusion flow cytometer (IGBMC Flow Cytometry Facility, Strasbourg, France).
453 Isolated LT-HSCs were at least 98% pure. 250 STING GOF or WT LT-HSCs from 6-weeks
454 old $CD45.2^{+}$ donor mice were i.v. injected with $5 \times 10^{5}$ supporting $CD45.1^{+}$ WT BM cells into
455 9-Gy lethally irradiated $CD45.1^{+}CD45.2^{+}$ WT hosts. The spleens of the mice were harvested 6
456 months after transplantation and the splenocytes analyzed by flow cytometry as described
457 above.
458
459 **Wild-type (WT) total bone marrow cells transplantations**
460 $1 \times 10^{6}$ WT total BM cells from 10 to 15-weeks old $CD45.1^{+}$ donor mice were i.v.
461 injected into 9-Gy lethally irradiated $CD45.2^{+}$ STING GOF or WT hosts. Mouse spleens were
462 harvested 6 months after transplantation and the splenocytes analyzed by flow cytometry as
463 described above.
464
465 **Statistical analysis**
466 All data are presented as means +/- SEMs. Statistical analyses were performed with
467 Prism 8.2.1 software (GraphPad). Statistical significance was calculated with the non-
468 parametric test of Mann-Whitney test, except for NFATc1 MFI ratio, where statistical
469 significance was calculated with Wilcoxon signed-rank test with a hypothetical value of 1 (see
470 details in each Figure legends).
471
472 **Acknowledgements**
473 We thank Fabrice Augé, Christian Galmiche, Delphine Lamon, Manon Lecointe, Fabien

Lhericel, Sophie Reibel-Foisset for excellent animal care. We thank Vincent Gies, Frédéric Gros, Aurélien Guffroy, Sophie Jung and Thierry Martin (INSERM UMR - S1109, Strasbourg University, France), Vincent Flacher and Christopher Mueller (CNRS UPR 3572, Institute of Molecular and Cellular Biology (IBMC), Strasbourg, France) for scientific discussions. We thank the Flow Cytometry facility of IGBMC (Illkirch, France) for cell sorting. This work was supported by the Hôpitaux Universitaires de Strasbourg (HUS), by the "Direction de la Recherche Clinique et de l'Innovation" (HUS) and by grants from Strasbourg University (UdS), by the Agence Nationale de la Recherche (ANR-14-CE14-0026-04, Lumugene; ANR-19-CE15-0028, LYMPHO-STING; and ANR-11-EQPX-022). The study was also supported by the Institut National de la Santé et de la Recherche Médicale (INSERM), by the Atip-Avenir, by government grants managed by the Agence National de la Recherche as part of the "Investment for the Future" program (Institut Hospitalo-Universitaire Imagine, grant ANR-10-IAHU-01, Recherche Hospitalo-Universitaire, grant ANR-18-RHUS-0010). Luigi D. Notarangelo is supported by the Division of Intramural Research, National Institute of Allergy and Infectious Diseases, National Institutes of Health.

489 **References**


490 1. A. Ablasser, Z. J. Chen, cGAS in action: Expanding roles in immunity and
491 inflammation. *Science* **363**, eaat8657 (2019).

492 2. K.-P. Hopfner, V. Hornung, Molecular mechanisms and cellular functions of cGAS–
493 STING signalling. *Nat Rev Mol Cell Biol* **21**, 501–521 (2020).

494 3. Y. Liu, *et al.*, Activated STING in a Vascular and Pulmonary Syndrome. *N Engl J Med*
495 **371**, 507–518 (2014).

496 4. N. Jeremiah, *et al.*, Inherited STING-activating mutation underlies a familial
497 inflammatory syndrome with lupus-like manifestations. *J. Clin. Invest.* **124**, 5516–5520
498 (2014).

499 5. Y. J. Crow, D. B. Stetson, The type I interferonopathies: 10 years on. *Nat Rev Immunol*
500 (2021).

501 6. M.-L. Frémond, *et al.*, Overview of STING-Associated Vasculopathy with Onset in
502 Infancy (SAVI) Among 21 Patients. *The Journal of Allergy and Clinical Immunology:*
503 *In Practice* **9**, 803-818.e11 (2021).

504 7. M.-L. Frémond, Y. J. Crow, STING-Mediated Lung Inflammation and Beyond. *J Clin*
505 *Immunol* **41**, 501–514 (2021).

506 8. C. David, M.-L. Frémond, Lung Inflammation in STING-Associated Vasculopathy with
507 Onset in Infancy (SAVI). *Cells* **11**, 318 (2022).

508 9. D. Bouis, *et al.*, Severe combined immunodeficiency in stimulator of interferon genes
509 (STING) V154M/wild-type mice. *Journal of Allergy and Clinical Immunology* **143**,
510 712-725.e5 (2019).

511 10. M. Motwani, *et al.*, Hierarchy of clinical manifestations in SAVI N153S and V154M
512 mouse models. *Proc. Natl. Acad. Sci. U.S.A.* **116**, 7941–7950 (2019).

513 11. J. D. Warner, *et al.*, STING-associated vasculopathy develops independently of IRF3 in
514 mice. *Journal of Experimental Medicine* **214**, 3279–3292 (2017).

515 12. H. Luksch, *et al.*, STING-associated lung disease in mice relies on T cells but not type
516 I interferon. *Journal of Allergy and Clinical Immunology* **144**, 254-266.e8 (2019).

517 13. B. G. Bennion, *et al.*, A Human Gain-of-Function STING Mutation Causes
518 Immunodeficiency and Gammaherpesvirus-Induced Pulmonary Fibrosis in Mice. *J*
519 *Virol* **93**, e01806-18 (2019).

520 14. G. R. Martin, *et al.*, Expression of a constitutively active human *STING* mutant in
521 hematopoietic cells produces an *Ifnar1* -dependent vasculopathy in mice. *Life Sci.*
522 *Alliance* **2**, e201800215 (2019).

523 15. H. Siedel, A. Roers, A. Rösen-Wolff, H. Luksch, Type I interferon-independent T cell
524 impairment in a Tmem173 N153S/WT mouse model of STING associated vasculopathy

525 with onset in infancy (SAVI). *Clinical Immunology* **216**, 108466 (2020).

526 16. B. G. Bennion, *et al.*, STING Gain-of-Function Disrupts Lymph Node Organogenesis
527 and Innate Lymphoid Cell Development in Mice. *Cell Reports* **31**, 107771 (2020).

528 17. K. M. Gao, M. Motwani, T. Tedder, A. Marshak-Rothstein, K. A. Fitzgerald,
529 Radioresistant cells initiate lymphocyte-dependent lung inflammation and IFNγ-
530 dependent mortality in STING gain-of-function mice. *Proc. Natl. Acad. Sci. U.S.A.* **119**,
531 e2202327119 (2022).

532 18. S. Cerboni, *et al.*, Intrinsic antiproliferative activity of the innate sensor STING in T
533 lymphocytes. *Journal of Experimental Medicine* **214**, 1769–1785 (2017).

534 19. M. F. Gulen, *et al.*, Signalling strength determines proapoptotic functions of STING.
535 *Nat Commun* **8**, 427 (2017).

536 20. J. Wu, *et al.*, STING-mediated disruption of calcium homeostasis chronically activates
537 ER stress and primes T cell death. *Journal of Experimental Medicine* **216**, 867–883
538 (2019).

539 21. A. R. Concepcion, *et al.*, The volume-regulated anion channel LRRC8C suppresses T
540 cell function by regulating cyclic dinucleotide transport and STING–p53 signaling. *Nat*
541 *Immunol* **23**, 287–302 (2022).

542 22. L. M. Ott De Bruin, *et al.*, Hypomorphic Rag1 mutations alter the preimmune repertoire
543 at early stages of lymphoid development. *Blood* **132**, 281–292 (2018).

544 23. E. J. Wherry, M. Kurachi, Molecular and cellular insights into T cell exhaustion. *Nat*
545 *Rev Immunol* **15**, 486–499 (2015).

546 24. L. M. McLane, M. S. Abdel-Hakeem, E. J. Wherry, CD8 T Cell Exhaustion During
547 Chronic Viral Infection and Cancer. *Annu. Rev. Immunol.* **37**, 457–495 (2019).

548 25. R. Labrosse, *et al.*, Aberrant T-cell exhaustion in severe combined immunodeficiency
549 survivors with poor T-cell reconstitution after transplantation. *Journal of Allergy and*
550 *Clinical Immunology* **151**, 260–271 (2023).

551 26. W. Dong, *et al.*, Exhaustion-like dysfunction of T and NKT cells in an X-linked severe
552 combined immunodeficiency patient with maternal engraftment by single-cell analysis.
553 *Int J Mol Med* **51**, 25 (2023).

554 27. E. J. Wherry, *et al.*, Molecular Signature of CD8+ T Cell Exhaustion during Chronic
555 Viral Infection. *Immunity* **27**, 670–684 (2007).

556 28. G. J. Martinez, *et al.*, The Transcription Factor NFAT Promotes Exhaustion of Activated
557 CD8 + T Cells. *Immunity* **42**, 265–278 (2015).

558 29. Y. Guo, *et al.*, Metabolic reprogramming of terminally exhausted CD8+ T cells by IL-
559 10 enhances anti-tumor immunity. *Nat Immunol* **22**, 746–756 (2021).

560 30. T. S. Sumida, *et al.*, Type I interferon transcriptional network regulates expression of
561 coinhibitory receptors in human T cells. *Nat Immunol* **23**, 632–642 (2022).

562 31. W. Seo, C. Jerin, H. Nishikawa, Transcriptional regulatory network for the
563 establishment of CD8+ T cell exhaustion. *Exp Mol Med* **53**, 202–209 (2021).

564 32. C. D. Surh, J. Sprent, Homeostasis of Naive and Memory T Cells. *Immunity* **29**, 848–
565 862 (2008).

566 33. I. Benoit-Lizon, *et al.*, CD4 T cell-intrinsic STING signaling controls the differentiation
567 and effector functions of $T_H$ 1 and $T_H$ 9 cells. *J Immunother Cancer* **10**, e003459
568 (2022).

569 34. E. F. McKinney, J. C. Lee, D. R. W. Jayne, P. A. Lyons, K. G. C. Smith, T-cell
570 exhaustion, co-stimulation and clinical outcome in autoimmunity and infection. *Nature*
571 **523**, 612–616 (2015).

572 35. C. U. Blank, *et al.*, Defining 'T cell exhaustion.' *Nat Rev Immunol* **19**, 665–674 (2019).

573 36. S. Terawaki, *et al.*, IFN-α Directly Promotes Programmed Cell Death-1 Transcription
574 and Limits the Duration of T Cell-Mediated Immunity. *The Journal of Immunology* **186**,
575 2772–2779 (2011).

576 37. E. B. Wilson, *et al.*, Blockade of Chronic Type I Interferon Signaling to Control
577 Persistent LCMV Infection. *Science* **340**, 202–207 (2013).

578 38. J. Wu, N. Dobbs, K. Yang, N. Yan, Interferon-Independent Activities of Mammalian
579 STING Mediate Antiviral Response and Tumor Immune Evasion. *Immunity* **53**, 115-
580 126.e5 (2020).

581 39. B. Jneid, *et al.*, Selective STING stimulation in dendritic cells primes antitumor T cell
582 responses. *Sci. Immunol.* **8**, eabn6612 (2023).

583 40. S. Dähling, *et al.*, Type 1 conventional dendritic cells maintain and guide the
584 differentiation of precursors of exhausted T cells in distinct cellular niches. *Immunity*
585 **55**, 656-670.e8 (2022).

586 41. F. Simonetta, *et al.*, Dynamics of Expression of Programmed Cell Death Protein-1 (PD-
587 1) on T Cells After Allogeneic Hematopoietic Stem Cell Transplantation. *Front.*
588 *Immunol.* **10**, 1034 (2019).

589 42. D. Kim, *et al.*, TopHat2: accurate alignment of transcriptomes in the presence of
590 insertions, deletions and gene fusions. *Genome Biol* **14**, R36 (2013).

591 43. C. Trapnell, *et al.*, Transcript assembly and quantification by RNA-Seq reveals
592 unannotated transcripts and isoform switching during cell differentiation. *Nat*
593 *Biotechnol* **28**, 511–515 (2010).

594 44. V. K. Mootha, *et al.*, PGC-1α-responsive genes involved in oxidative phosphorylation
595 are coordinately downregulated in human diabetes. *Nat Genet* **34**, 267–273 (2003).

596 45. A. Subramanian, *et al.*, Gene set enrichment analysis: A knowledge-based approach for
597 interpreting genome-wide expression profiles. *Proc. Natl. Acad. Sci. U.S.A.* **102**, 15545–
598 15550 (2005).

599

600 **FIGURES**

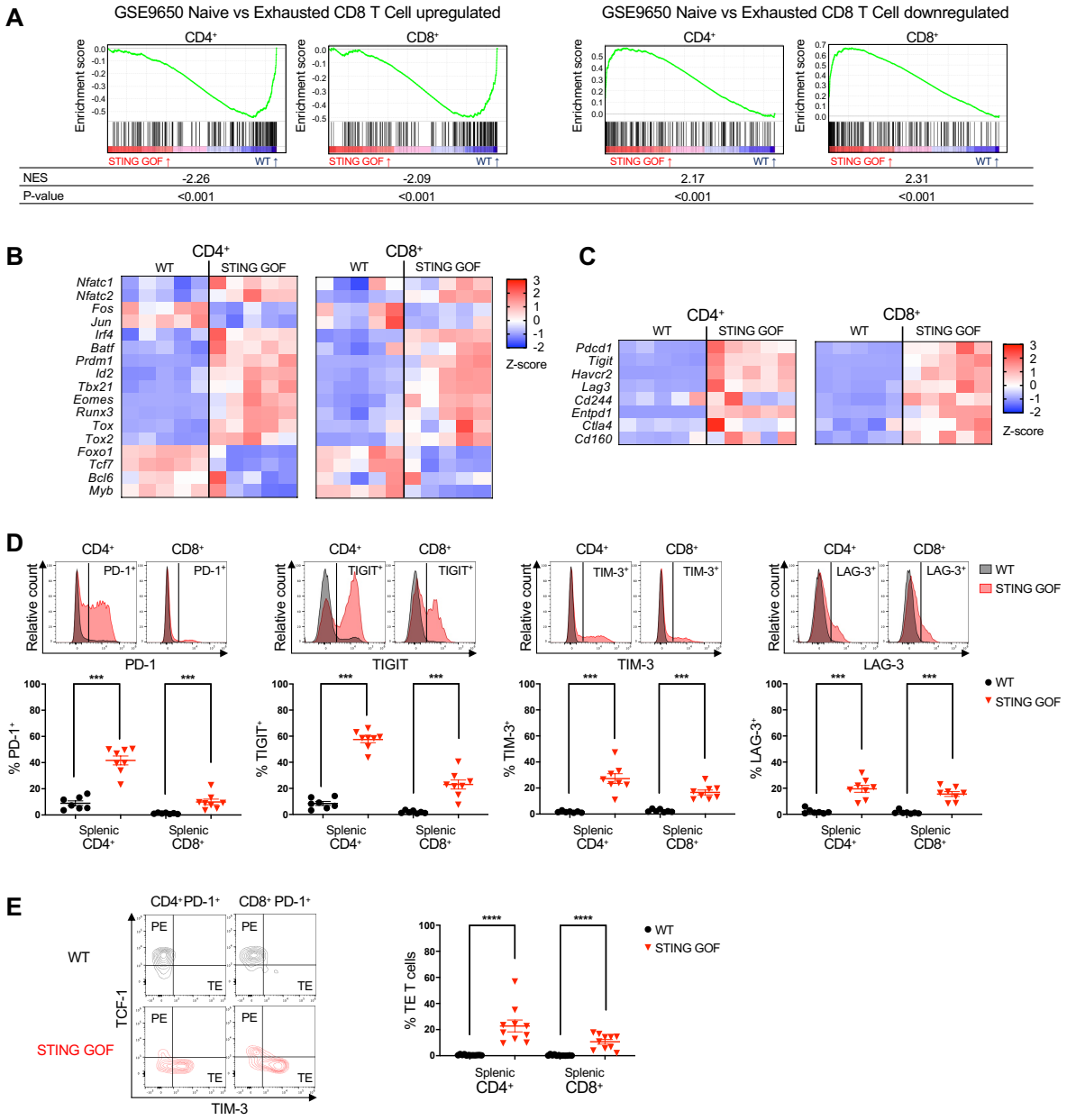


601

602 **Figure 1. Splenic CD4+ and CD8+ T cells from STING GOF mice display an exhausted**
603 **phenotype.**

604 **(A-C)** Analysis of RNA-seq performed on sorted splenic CD4$^+$ or CD8$^+$ T cells from STING
605 GOF mice (n=5) and their WT littermate controls (n=5). **(A)** Gene Set Enrichment Analysis
606 (GSEA) of the signatures of genes upregulated or downregulated in naive versus exhausted
607 CD8$^+$ T cells (GSE9650) among genes deregulated in STING GOF versus WT CD4$^+$ or CD8$^+$
608 T cells. Enrichment plots, normalized enrichment score (NES) and nominal p-value (p-value)
609 are shown for each analysis. **(B)** Heatmap representing T cell exhaustion/dysregulated
610 transcription factors mRNA expression (Z-score) by CD4$^+$ or CD8$^+$ T cells in STING GOF mice
611 compared to WT mice. **(C)** Heatmap representing inhibitory receptors mRNA expression (Z-
612 score) by CD4$^+$ or CD8$^+$ T cells in STING GOF and WT mice. **(D-E)** Immunophenotyping of
613 splenic T cells from STING GOF mice and their WT littermate controls by flow cytometry. **(D)**

614 Proportion of PD-1-, TIGIT-, TIM-3- and LAG-3-expressing cells among $CD4^+$ or $CD8^+$ T
615 cells. Representative histograms are shown. **(E)** Proportion of terminally exhausted (TE) T cells
616 among $CD4^+$ or $CD8^+$ T cells. Representative contour plots are shown. Each data point
617 corresponds to one mouse; mean ± SEM are shown per population for seven to twelve mice
618 from multiple independent experiments. Statistical significances are calculated with two-tailed
619 Mann-Whitney test: ***, $P < 0.001$; ****, $P < 0.0001$.

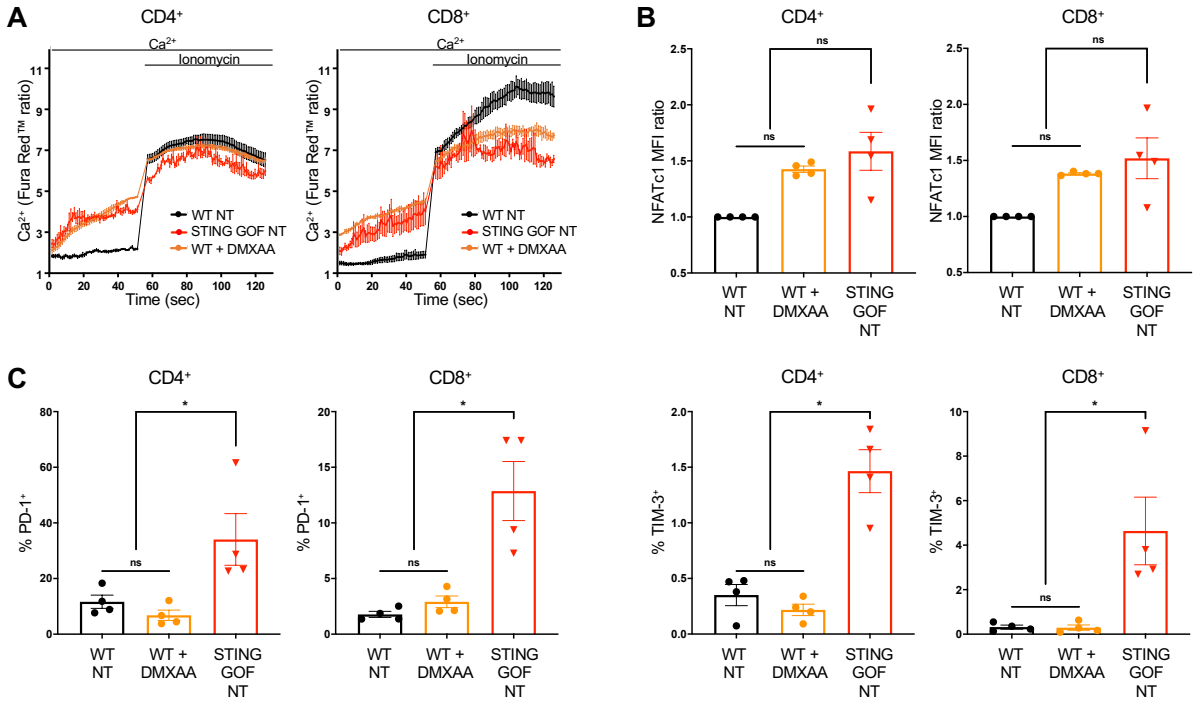


620

621 **Figure 2. $Ca^{2+}$-NFAT pathway is activated by STING, but is not sufficient to induce T cell**
622 **exhaustion.**

623 **(A-C)** Splenic WT splenocytes were treated *in vitro* with DMXAA (10 µg/mL) and compared
624 to untreated (NT) WT and STING GOF splenocytes. After 4 hours (calcium levels
625 measurement) or 24 hours (immunophenotyping), cells were analyzed by flow cytometry. **(A)**
626 Relative cytosolic $Ca^{2+}$ levels monitored by Fura Red™ ratio in $CD4^+$ or $CD8^+$ T cells
627 Splenocytes were treated, recorded, and plotted as in Fig. S3C. Each data point represents the
628 mean of three independent experiments, and their error bars the SEM. **(B)** Ratio of total
629 NFATc1 MFI in $CD4^+$ or $CD8^+$ T cells. Ratio was normalized on the corresponding WT
630 untreated control. **(C)** Proportion of PD-1- and TIM-3-expressing cells among $CD4^+$ or $CD8^+$
631 T cells. Each data point corresponds to one mouse; mean ± SEM are shown per population for
632 four mice from four independent experiments. For NFATc1 MFI ratio, statistical significances
633 are calculated with Wilcoxon signed-rank test with a hypothetical value of 1: ns, $P > 0.05$. For
634 PD-$1^+$ and TIM-$3^+$ proportions, statistical significances are calculated with two-tailed Mann-
635 Whitney test: ns, $P > 0.05$; *, $P < 0.05$.

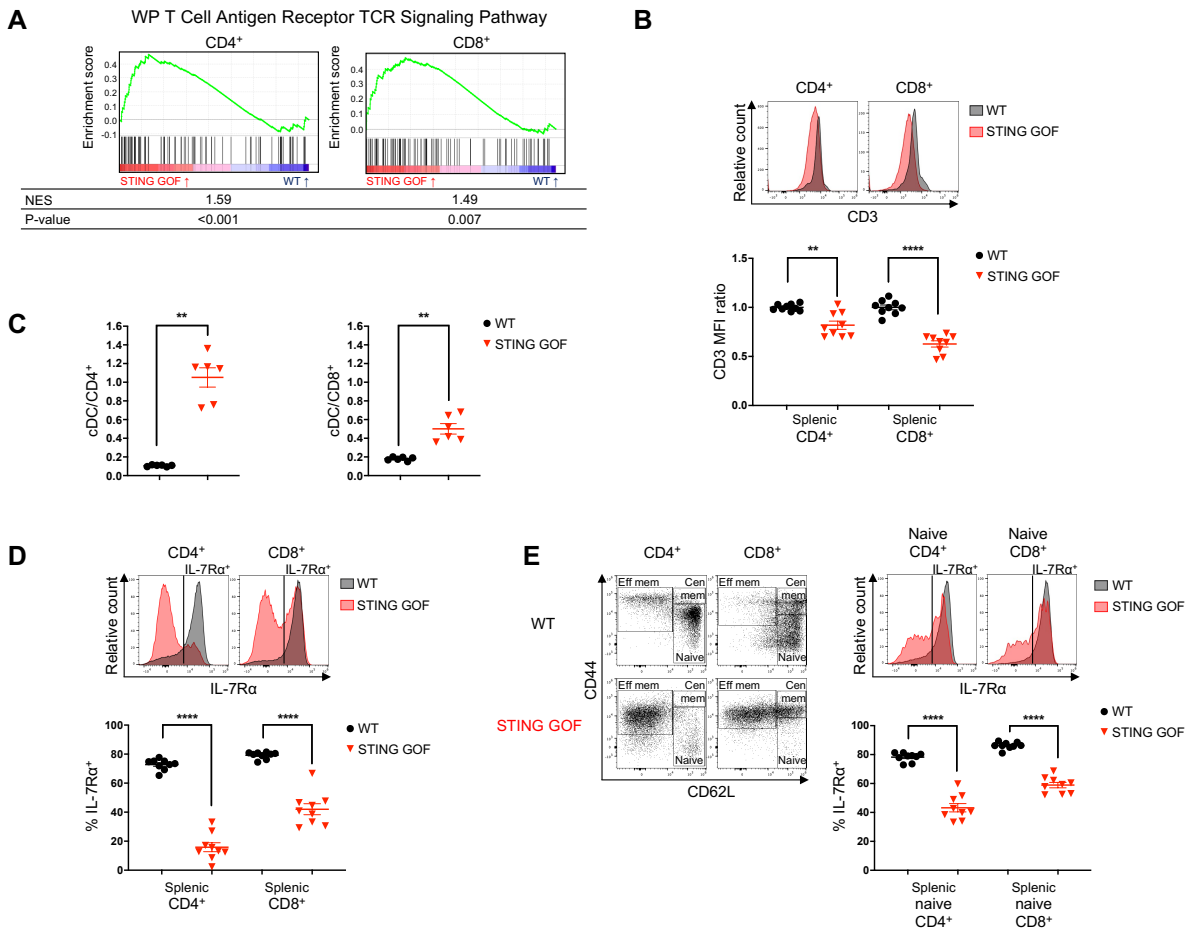


**Figure 3. STING GOF T cells displayed features of TCR and IL-7R engagement mediated by the lymphopenic environment.**

**(A)** GSEA of the TCR pathway signature (WP) among genes deregulated in STING GOF versus WT CD4$^+$ or CD8$^+$ T cells. Enrichment plots, normalized enrichment score (NES) and nominal p-value (p-value) are shown for each analysis. **(B)** Ratio of CD3 mean fluorescence intensity (MFI) on splenic CD4$^+$ or CD8$^+$ T cells from STING GOF mice and their WT littermate controls. Ratio was normalized on the mean of WT controls of each analysis. Representative histograms are shown. **(C)** Ratio of cDCs absolute number per CD4$^+$ or CD8$^+$ T cells numbers from the spleen of 4-week-old mice. **(D-E)** Proportion of IL-7Rα-expressing cells among splenic total **(D)** and naive (CD44$^-$CD62L$^+$) **(E)** CD4$^+$ or CD8$^+$ T cells from STING GOF mice and their WT littermate controls. Gating strategy of naive T cells and representative histograms are shown. Each data point corresponds to one mouse; mean ± SEM are shown per population for six to nine mice from multiple independent experiments. Statistical significances are calculated with two-tailed Mann-Whitney test: **, $P < 0.01$; ****, $P < 0.0001$.

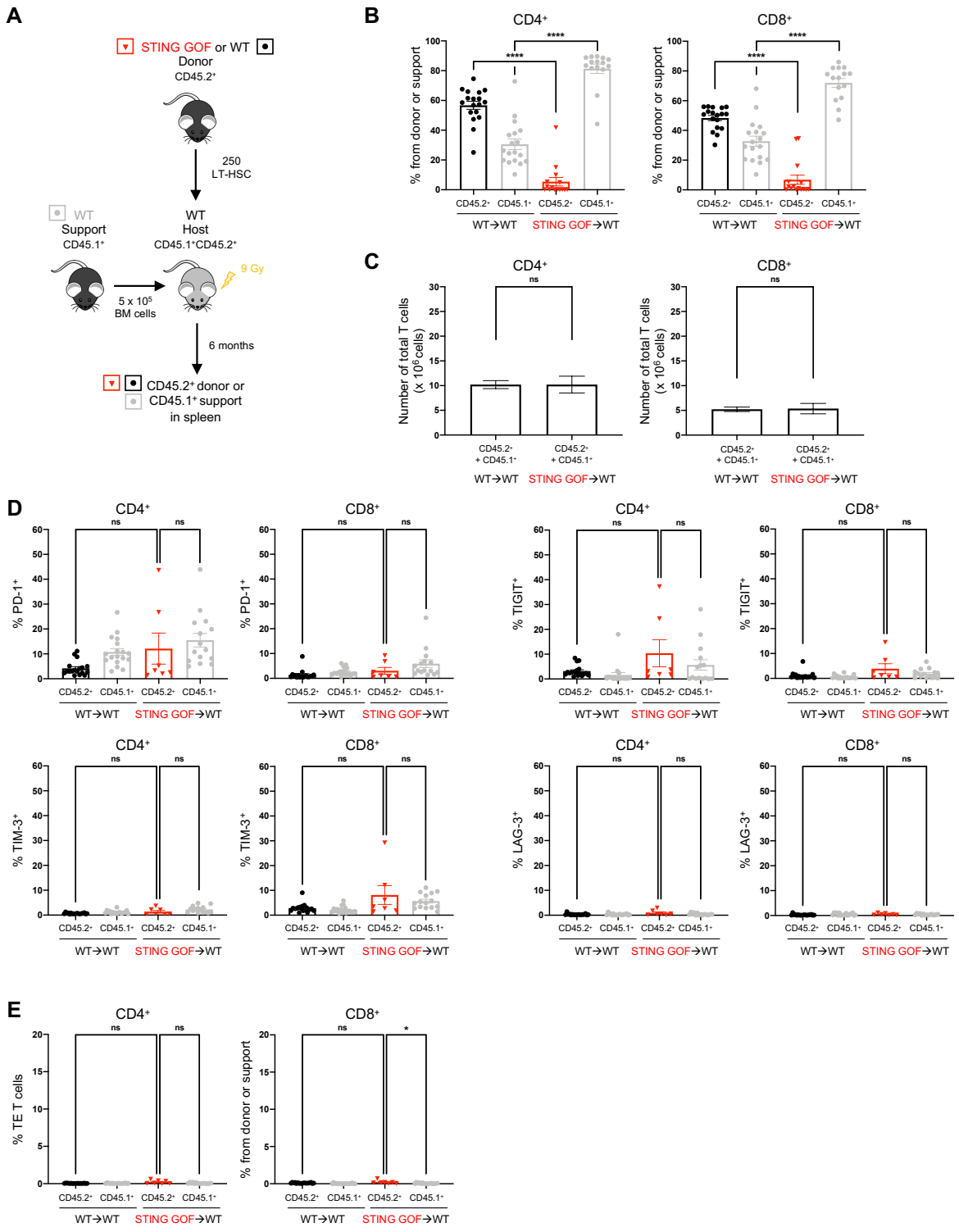


**Figure 4. T cell exhaustion phenotype of STING GOF T cell is reversed in a non-lymphopenic environment.**

**(A-E)** LT-HSCs from STING GOF mice and their WT littermate controls (CD45.2$^+$) were transplanted with WT BM supportive cells (CD45.1$^+$) in WT irradiated hosts to generate STING GOF→WT and WT→WT mice. 6 months later, spleens were assessed for T cell reconstitution and immunophenotyping. **(A)** Strategy of LT-HSCs transplantations with supportive BM cells. **(B)** Proportion of cells derived from donor (CD45.2$^+$) LT-HSCs or WT BM supportive cells

659 (CD45.1$^{+}$) among splenic CD4$^{+}$ or CD8$^{+}$ T cells from STING GOF→WT and WT→WT mice.
660 **(C)** Absolute numbers of total (CD45.2$^{+}$ and CD45.1$^{+}$) splenic CD4$^{+}$ or CD8$^{+}$ T cells from
661 STING GOF→WT and WT→WT mice. **(D)** Proportion of PD-1-, TIGIT-, TIM-3- and LAG-
662 3-expressing cells among splenic CD4$^{+}$ or CD8$^{+}$ T cells **(E)** Proportion of terminally exhausted
663 (TE) T cells among splenic CD4$^{+}$ or CD8$^{+}$ T cells. Each data point corresponds to one mouse;
664 mean ± SEM are shown per population for seven to eighteen mice from multiple independent
665 experiments. Statistical significances are calculated with two-tailed Mann-Whitney test: ns, $P > 0.05$; *, $P < 0.05$; ****, $P < 0.0001$.

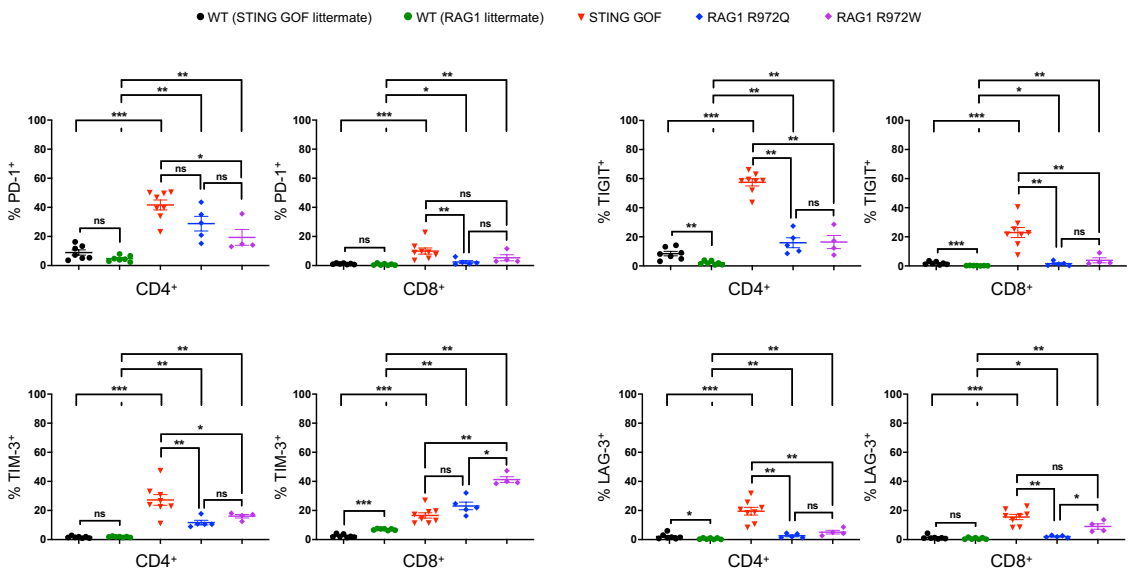


**Figure 5. Mice carrying Rag1 hypomorphic mutations also display lymphopenia-associated T cell exhaustion.**

Proportion of PD-1-, TIGIT-, TIM-3- and LAG-3-expressing cells among splenic $CD4^+$ or $CD8^+$ T cells from hypomorphic RAG1 R972Q and R972W mice and their WT littermate controls by flow cytometry. Data were compared with previous results obtained from STING GOF mice and their WT littermate controls. Each point corresponds to one mouse; mean ± SEM are shown per population for four to twelve mice from multiple independent experiments. Statistical significances are calculated with two-tailed Mann-Whitney test: ns, $P > 0.05$; *, $P < 0.05$; **, $P < 0.01$; ***, $P < 0.001$.